Michigan State University

National Superconducting Cyclotron Laboratory

TRANSITIONS IN NUCLEAR DISASSEMBLY AS VIEWED BY FRAGMENT CHARGE CORRELATIONS.

N.T.B. STONE, W. J. LLOPE, and G.D. WESTFALL

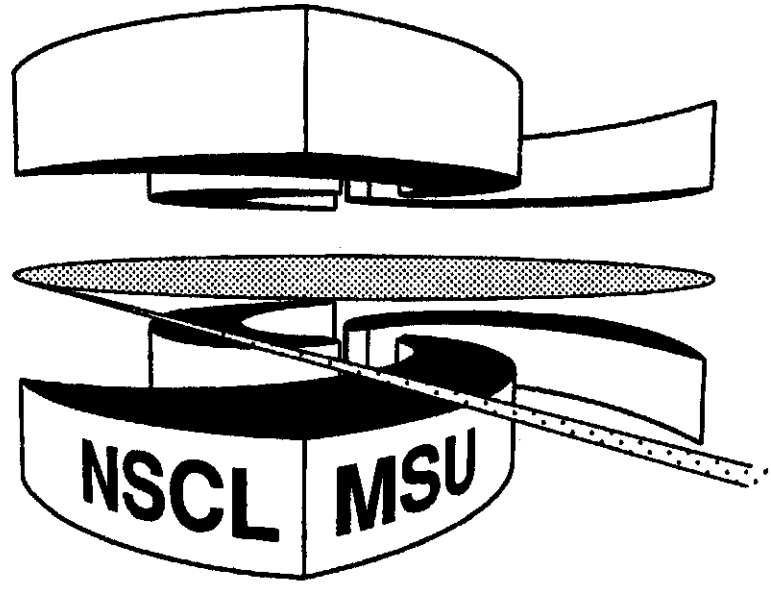

MSUCL-916

March 1994

Transitions in nuclear disassembly as viewed by fragment charge correlations.

N.T.B. Stone[1,2], W.J. Llope[1,†], and G.D. Westfall[1,2]

[1]National Superconducting Cyclotron Laboratory, Michigan State University, East Lansing, MI 48824-1321

[2]Department of Physics and Astronomy, Michigan State University, East Lansing, MI 48824-1321

PACS Number: 25.70.Pq

Abstract

Central heavy-ion collisions in four nearly symmetric entrance channels, $^{20}Ne+^{27}Al$, $^{40}Ar+^{45}Sc$, $^{87}Kr+^{93}Nb$, and $^{129}Xe+^{139}La$, have been studied systematically over a wide range of intermediate beam energies. The relative sizes of the three largest fragments in the central events are studied using charge Dalitz plots. Two observables, D_{cent} and D_{edge}, are introduced to quantify the distributions of the central events in such plots, allowing the inference of the predominant disassembly mechanisms leading to these events. For increasing beam energies, transitions from sequential binary disassembly to multifragmentation are observed at ~50 and ~30 MeV/nucleon in the $^{40}Ar+^{45}Sc$ and $^{129}Xe+^{139}La$ entrance channels, respectively. The results for the central $^{20}Ne+^{27}Al$($^{87}Kr+^{93}Nb$) reactions are consistent with the trends observed in the central $^{40}Ar+^{45}Sc$($^{129}Xe+^{139}La$) reactions over the same range of beam energies.

†Present Address: Bonner Nuclear Laboratory, Rice University, Houston, TX 77251-1892.

Particular trends in the slopes and functional form of the charge distributions of fragments emitted following central heavy-ion collisions have been noted [1, 2, 3] as strong signals for liquid-gas phase transitions in excited nuclei [1, 4]. A relatively shallow power-law charge distribution for charges $1 \leq Z \lesssim 20$ is expected at the transitional excitation energy, as compared to steeper exponential distributions at energies both above and below. However, a power-law behavior of the fragment charge distributions may also result from averaging over impact parameters or excitation energies [2, 5], imitating the expected signal of a liquid-gas phase transition. In this Letter, we propose observables based on the relative sizes of the three largest fragments following a systematic study of central ^{20}Ne+^{27}Al, ^{40}Ar+^{45}Sc, ^{84}Kr+^{93}Nb, and ^{129}Xe+^{139}La reactions. These observables, D_{cent} and D_{edge}, are extracted from charge Dalitz plots [6], and used to evaluate the importance of sequential binary (SB) [7, 8, 9, 10, 11] and multifragmentation (MF) [11, 12] disassembly mechanisms in the small impact parameter events. The observation of a transition from SB disassembly to MF for increasing beam energies would be suggestive of the transition from liquid to liquid-gas coexistence phases, i.e. the "cracking" transition, that has been predicted by several models [12, 13].

Each central event is assigned a location in an equilateral triangle of unit altitude by equating the distances to the three sides of the triangle to the relative charges of the three largest fragments, i.e. $Z_i' = Z_i/Z_{sum}$, where $Z_1(Z_3)$ is the charge of the largest(third largest) fragment and $Z_{sum} = \sum_{i=1}^{3} Z_i$. We define the distance from each entry to the geometric center of the triangle,

$$D_{cent} = \sqrt{(Z_1' \tan 30^\circ + Z_2'/\cos 30^\circ - \frac{1}{\sqrt{3}})^2 + (Z_1' - \frac{1}{3})^2}, \quad (1)$$

and the perpendicular distance to the nearest edge, $D_{edge} = Z_3'$. Events with three or more nearly equally sized largest fragments will populate the center of the triangle ($D_{cent} < D_{edge}$), while those with one large fragment and two smaller, or two large fragments and one smaller, will populate the corners or sides of the triangle, respectively ($D_{cent} > D_{edge}$). These possibilities can be assumed to be populated predominantly by specific nuclear disassembly mechanisms [6].

We classify as sequential binary those disassembly mechanisms involving a cascade of two-body decay steps, in which each step is independent and may involve (a)symmetric binary fission [7, 8], (a)symmetric ternery fission [9], or evaporation [7, 10]. Over the course of a purely evaporative SB decay, the probability of emitting large fragments decreases due to the increasing importance of the Coulomb and angular momentum barriers. The three largest charges in final states produced in such SB decays would thus be expected to consist of one larger fragment and two smaller ones. A binary or ternery fission step in the SB decay cascade would result in the emission of two larger fragments and one smaller one. Disassembly leading to three similarly sized largest fragments has been noted as a signal for the process known as multifragmentation [11, 12]. For some sample of events, we therefore make the assignment that $\langle D_{cent} \rangle > \langle D_{edge} \rangle$ implies the predominance of SB disassembly, while $\langle D_{cent} \rangle < \langle D_{edge} \rangle$ implies multifragmentation. In the central events with $\langle D_{cent} \rangle > \langle D_{edge} \rangle$, a population near the corners of the charge Dalitz triangles implies asymmetric fission or sequential evaporative decays, while one near the sides implies symmetric binary or ternery fission [6].

The reactions studied were ^{20}Ne+^{27}Al at beam energies of 55, 75, 95, 105, 115, 125, 135, and 140 MeV/nucleon; ^{40}Ar+^{45}Sc at 15, 25, 35, 45, 65, 75, 85, 95, 105, and 115 MeV/nucleon; ^{84}Kr+^{93}Nb at 35, 45, 55, 65, and 75 MeV/nucleon; and ^{129}Xe+^{139}La at 25, 30, 35, 40, 45, 50, 55, and 60 MeV/nucleon. The beams were obtained from the K1200 cyclotron at the National Superconducting Cyclotron Laboratory, and all of the data were collected using the MSU 4π Array

[14] with a minimum bias trigger (two discriminator hits). The fragment charges were well resolved over the range $1 \leq Z \leq 15$ in the $^{20}Ne+^{27}Al$ and $^{84}Kr+^{93}Nb$ entrance channels, and $1 \leq Z \leq 18$ in the $^{40}Ar+^{45}Sc$ and $^{129}Xe+^{139}La$ entrance channels. Further information concerning the apparatus and data collection can be found in Refs. [14, 15]. The distortions to the present results that are caused by the inefficiencies in experimental measurement were studied using events generated by model codes and a software replica of the detection system. These are discussed as appropriate below.

The total mass and excitation energy of the excited systems formed for each reaction are constrained via the selection of the most central collisions. Separate impact parameter cuts allowing the ~10% most central of the minimum bias events were placed on a number of different variables. These include the total number of charged particles measured in an event (N_c), the total number of protons (N_p), the total charge in hydrogen and helium fragments (Z_{lcp}), the total transverse kinetic energy (KE_T), and the total charge of all particles in a software gate centered at mid-rapidity (Z_{MR}). The variables KE_T and Z_{MR} are defined as in Ref. [16]. Autocorrelations between the present relative charge observables and each of these centrality variables were investigated via the comparison of the widths of these observables in the events selected by the ~10% cuts on each of these centrality variables separately. Such autocorrelations result in a significant suppression of these widths, as compared to those resulting from cuts on non-autocorrelating centrality variables. The widths of the distributions of Z_1, Z_2, and Z_3 resulting from cuts on N_c, N_p, and Z_{lcp} were found to be suppressed by as much as a factor of two relative to the corresponding distributions following small impact parameter cuts on the variables KE_T and Z_{MR}. The widths of the D_{cent} and D_{edge} distributions were also suppressed following cuts on these three variables. Therefore, the centrality variables N_c, N_p, and Z_{lcp}, are significantly autocorrelated with the present relative charge observables. Two-dimensional small impact parameter cuts based on the variables KE_T and Z_{MR} will therefore be employed, which allow the 4-8% most central of the minimum bias events. According to approximate geometrical arguments, these events have average impact parameters $\langle b \rangle \lesssim 0.25 b_{max}$, where b_{max} is the sum of the radii of the projectile and target nucleus.

The average values of D_{cent} (with points) and D_{edge} (without points) in the selected central events are depicted in Figure 1 for all reactions. The solid lines depict these average distances for the events selected by the two-dimensional small impact parameter cut on KE_T and Z_{MR}, while the dashed(dot-dashed) lines correspond to the events passing one-dimensional cuts on $KE_T(Z_{MR})$ alone. For the lowest beam energies in both the $^{40}Ar+^{45}Sc$ and $^{129}Xe+^{139}La$ systems, $\langle D_{cent} \rangle > \langle D_{edge} \rangle$ in the central events. This implies an overall asymmetry in the charges of the largest three fragments in these events, and is thus consistent with a SB disassembly mechanism. These events are predominantly near the corners of the charge Dalitz triangles, implying that asymmetric fission or sequential evaporation decays are more common than those involving a symmetric binary or ternery fission. For higher beam energies in these entrance channels, as well as for all of the beam energies in the $^{20}Ne+^{27}Al$ and $^{87}Kr+^{93}Nb$ entrance channels, $\langle D_{cent} \rangle < \langle D_{edge} \rangle$. The largest three fragments in the final state are thus similarly sized, which implies multifragmentation.

A beam energy that is transitional between SB and MF disassembly is defined at the crossing of the lines interpolated from the points shown in Figure 1. The transitional beam energies extracted from Figure 1 for the central $^{40}Ar+^{45}Sc$ and $^{129}Xe+^{139}La$ reactions are ~50 and ~33 MeV/nucleon, respectively. The results for the central $^{87}Kr+^{93}Nb$ reactions are similar to those for the central $^{129}Xe+^{139}La$ reactions, implying a transitional beam energy somewhere in the range of 30-35 MeV/nucleon for this system. The average distances in the central $^{20}Ne+^{27}Al$ reactions are generally consistent with those observed in the $^{40}Ar+^{45}Sc$ reactions at the same beam energies. The

transitional beam energies are 3-5 MeV/nucleon higher in the samples of events from the two one-dimensional cuts (dashed and dot-dashed lines) than those obtained following the two-dimensional cut (solid lines). The values of $\langle D_{cent} \rangle$ and $\langle D_{edge} \rangle$ appear to reach asymptotic values within a few tens of MeV/nucleon above the transitional beam energies.

It is noted, however, that there are hidden constraints on the present method. For example, events characterized by a low value of Z_{sum} cannot, by definition, populate the extreme corners or sides of the Dalitz triangles. Indeed, there are well-defined maximum and minimum possible values of D_{cent} and D_{edge} for each value of Z_{sum}. These extrema are shown for D_{edge} in Figure 2 as the solid lines (analogous limits apply for D_{cent}). As Z_{sum} is decreased, the range of possible values of D_{edge} decreases, and this range tends towards larger values of D_{edge}. It is therefore possible that the crossings noted in Figure 1 are simply an artifact of similarly beam energy dependent decreases in the average values of Z_{sum}. The values of Z_{sum} averaged over beam energies in each entrance channel are 6.7, 9.9, 15.7, and 19.0, for the ^{20}Ne+^{27}Al through ^{129}Xe+^{139}La systems, which correspond to 29%, 25%, 20%, and 17% of the total entrance channel charge. The percentage standard deviations about these average values over the different beam energies in each entrance channel are 8%, 12%, 3%, and 7%. Thus, $\langle Z_{sum} \rangle$ is only weakly dependent on the beam energy in each entrance channel, so that the transitions noted in Figure 1 cannot simply be an artifact of decreases in $\langle Z_{sum} \rangle$ for increasing beam energies. The average values of D_{edge} are also plotted in this Figure for three representative beam energies in each entrance channel. These reveal a dependence of D_{edge} (and D_{cent}) on Z_{sum} that generally follows the shape of the region allowed by definition. For $3 \leq Z_{sum} \leq 5$, there is only one allowed value of D_{edge} (and D_{cent}). While no relative charge information can be extracted for $3 \leq Z_{sum} \leq 5$, central events with relatively small values of Z_{sum} are nonetheless interesting, as they indicate the presence of events in which no large fragments were observed, implying the rather complete vaporization of the system.

It is important to consider also the constraints on the present observables that are imposed by the inefficiencies of the detection system. The most obvious constraint of this kind results from the maximum charge that could be detected, which was ~15 for the ^{20}Ne+^{27}Al and ^{87}Kr+^{93}Nb reactions, and ~18 for the ^{40}Ar+^{45}Sc and ^{129}Xe+^{139}La reactions. The effect of this limit is to decrease the sensitivity of the present observables for large values of Z_{sum}. Specifically, as the values of Z_1 and Z_2 approach the maximum detectable charge, the number of possible permutations of Z_1, Z_2, and Z_3 having the same measured Z_{sum} decreases. This leads to a situation similar to that for $3 \leq Z_{sum} \leq 5$, where the limited range of possible values for D_{cent} and D_{edge} reduces their sensitivity. In Figure 2, the values of $\langle D_{edge} \rangle$ manifest fairly abrupt changes at roughly the maximum detected charge plus two, and twice that maximum plus one, corresponding to the detection of such large charges in coincidence with protons.

The values of $\langle D_{cent} \rangle$ and $\langle D_{edge} \rangle$ for the central events with $6 \leq Z_{sum} \leq 17$ for the ^{20}Ne+^{27}Al and ^{87}Kr+^{93}Nb entrance channels, and $6 \leq Z_{sum} \leq 20$, for the ^{40}Ar+^{45}Sc and ^{129}Xe+^{139}La entrance channels, are depicted in Figure 3. This gate on Z_{sum} allows those central events for which the present charge observables are not affected by the limiting maximum detectable charge. These curves indicate the same transitional behavior as shown in Figure 1, although at slightly lower beam energies: ~47 and ~29 MeV/nucleon for the ^{40}Ar+^{45}Sc and ^{129}Xe+^{139}La entrance channels, respectively.

A more complete investigation of the effects of the experimental acceptance involves the generation of software events, and the comparison of the present relative charge observables in these events with and without filtering by a software replica of the apparatus. The filter code includes

a complete description of the geometry and the kinetic energy thresholds. Multiple hits in individual detector elements are treated in consistency with the templates used to calibrate all of the experimental data. Separate samples of events were generated with the Berlin code [17], each at a specified excitation energy, in a system expected to be common in the present central ^{40}Ar+^{45}Sc reactions (Z~31, A~68). The upper two frames in Figure 4 depict $\langle Z_{sum} \rangle$ and $\langle D_{cent} \rangle$ after each of these samples of events is boosted from the center of momentum frame into the laboratory, and then filtered, for beam energies in the range of 25 to 105 MeV/nucleon. The events were generated at excitation energies of 2 (solid squares), 4, 6, 8, 10, 12, 16, and 20 (open crosses) MeV/nucleon. The filtered $\langle Z_{sum} \rangle$ and $\langle D_{cent} \rangle$ show only a very weak dependence on the magnitude of the boost into the laboratory for all of the samples of generated events. The crossings noted in Figures 1 and 3 are therefore not the result of a strong beam energy dependence of the experimental acceptance.

The solid curves in the lower frame in Figure 4 depict the excitation energy dependence of $\langle D_{cent} \rangle$ (with points) and $\langle D_{edge} \rangle$ (without points) for the unfiltered Berlin events. The unfiltered Berlin events evolve from the corners to the center of the charge Dalitz triangles, and exhibit a crossing excitation energy near 6 MeV/nucleon. Boltzmann-Uehling-Uehlenbeck (BUU) calculations are one means of specifying the relationship between the beam energy and the average excitation energy for central collisions. These calculations were performed as described in Ref. [18], and the predicted relationship between the beam and excitation energies is visible by comparing the upper and lower abscissa in this lower frame. The dotted lines in this frame depict the values of $\langle D_{cent} \rangle$ and $\langle D_{edge} \rangle$ following the boosting and filtering of the generated events assuming this relationship. The apparent crossing (beam) energy is only weakly affected by the imposition of the experimental inefficiencies via the software filter. The major effect is to reduce the apparent asymmetry of the three largest charges for asymmetric events, i.e. those in the SB region.

This letter has described a method of evaluating the importance of the specific disassembly mechanisms in a comprehensive set of central heavy-ion reactions using charge Dalitz plots. Small impact parameter collisions were selected using two-dimensional cuts on centrality variables that do not autocorrelate with the relative charge distributions. The observables D_{cent} and D_{edge} were introduced for the purpose of quantifying the distribution of events in the charge Dalitz triangles for each reaction. The constraints imposed on these observables, by definition and by the inefficiencies in the detection system, were shown not to affect our conclusions. Transitions from sequential binary disassembly to multifragmentation were observed in the central ^{40}Ar+^{45}Sc and ^{129}Xe+^{139}La entrance channels at beam energies of ~50 and ~30 MeV/nucleon, respectively. The results for the central ^{20}Ne+^{27}Al (^{84}Kr+^{93}Nb) reactions are consistent with the trends noted for the central ^{40}Ar+^{45}Sc(^{129}Xe+^{139}La) reactions over a more limited range of available beam energies.

We gratefully acknowledge the contributions of the MSU 4π Group during the data collection. The work is supported by the U.S. National Science Foundation under Grants No. PHY 89-13815 and PHY 92-14992.

References

[1] M.E. Fisher, Physics (Long Island City, NY) **3**, 255 (1967).

[2] W. Bauer, Phys. Rev. C **38**, 1297 (1988), and references therein.

[3] X. Campi, Phys. Lett. **B208**, 351 (1988);
D. Stauffer, Phys. Rep. **54**, 1 (1979);
A.S. Hirsch *et al.*, Phys. Rev. C **29**, 508 (1984);
J.E. Finn *et al.*, Phys. Rev. Lett. **49**, 1321 (1982).

[4] A.L. Goodman, J.I. Kapusta, and A.Z. Mekjian, Phys. Rev. C **30**, 851 (1984);
A.D. Panagiotou *et al.*, Phys. Rev. Lett. **52**, 496 (1984).

[5] J. Aichelin *et al.*, Phys. Rev. C **37**, 2451 (1988);
T. Li *et al.*, Phys. Rev. Lett. **70**, 1924 (1993).

[6] P. Kreutz *et al.*, Nucl. Phys. **A556**, 672 (1993);
P. Roussel-Chomaz *et al.*, Nuc. Phys. **A551**, 508 (1993);
G. Bizard *et al.*, Phys. Lett. **B302**, 162 (1993);
M. Colonna *et al.*, Phys. Lett. **B283**, 180 (1992).

[7] C. Barbagallo, J. Richert, and P. Wagner, Z. Phys. A **324**, 97 (1986);
R.J. Charity *et al.*, Nucl. Phys. **A483**, 371 (1988).

[8] G. Casini *et al.*, Phys. Rev. Lett. **71**, 2567 (1993);
H. Delagrange *et al.*, Z. Phys. A. **323**, 437 (1986).

[9] K. Siwek-Wilczynska *et al.*, Phys. Rev. C **48**, 228 (1993);
M. Sowiński *et al.*, Z. Phys. A. **324**, 87 (1986).

[10] F. Pühlhofer, Nucl. Phys. **A280**, 267 (1977).

[11] L.G. Moretto and G.J. Wozniak, Ann. Rev. Nucl. Part. Sci. (May, 1993).

[12] J.P. Bondorf *et al.*, Nucl. Phys. **A448**, 753 (1986), and references therein;
A.S. Botvina *et al.*, Nucl. Phys. **A475**, 663 (1987);
D.H.E. Gross, Proj. Part. Nucl. Phys. **30**, 155 (1993), and references therein.

[13] D.H.E. Gross and H. Massmann, Nucl. Phys. **A471**, 339c (1987).

[14] G.D. Westfall *et al.*, Nuc. Inst. and Meth. **A238**, 347 (1985).

[15] G.D. Westfall *et al.*, Phys. Rev. Lett. **71**, 1986 (1993).

[16] L. Phair *et al.*, Nucl. Phys. **A548**, 489 (1992).

[17] X.-Z. Zhang *et al.*, Nucl. Phys. **A461**, 668 (1987), and references therein.

[18] C.M. Mader, Ph.D. Thesis, Michigan State University, 1993 (unpublished); D.R. Bowman *et al.*, Phys. Rev. C **46**, 1834 (1992).

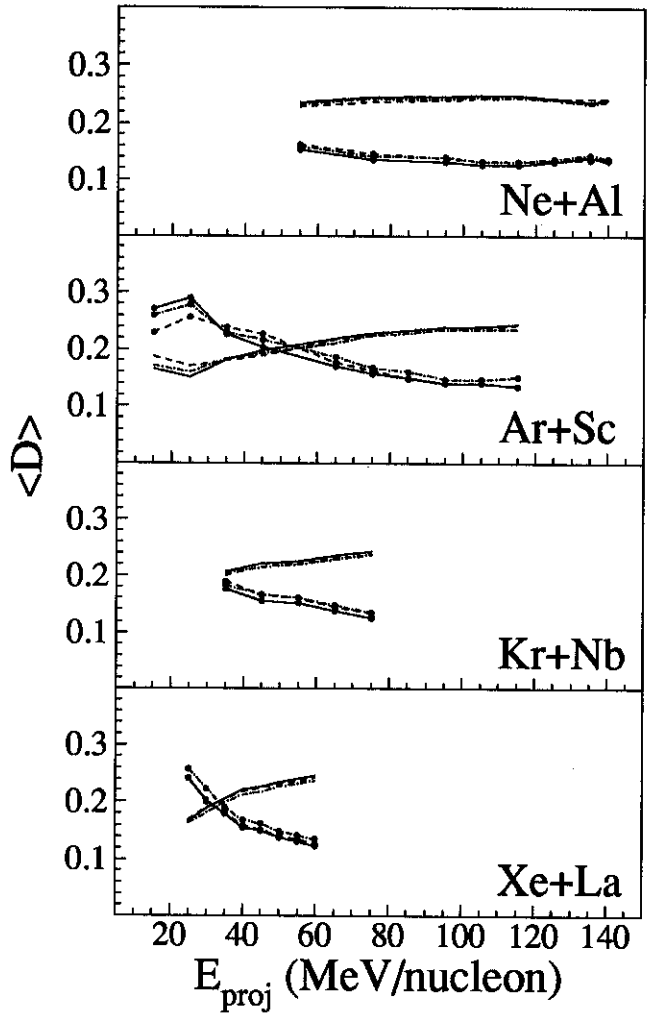

Figure 1: The average values of D_{cent} (with points) and D_{edge} (without points) in the central events versus the projectile energy. The solid lines depict the results for events selected by the two-dimensional cut on KE_T and Z_{MR}, while the dashed(dot-dashed) lines correspond to events selected by a one-dimensional cut on $KE_T(Z_{MR})$.

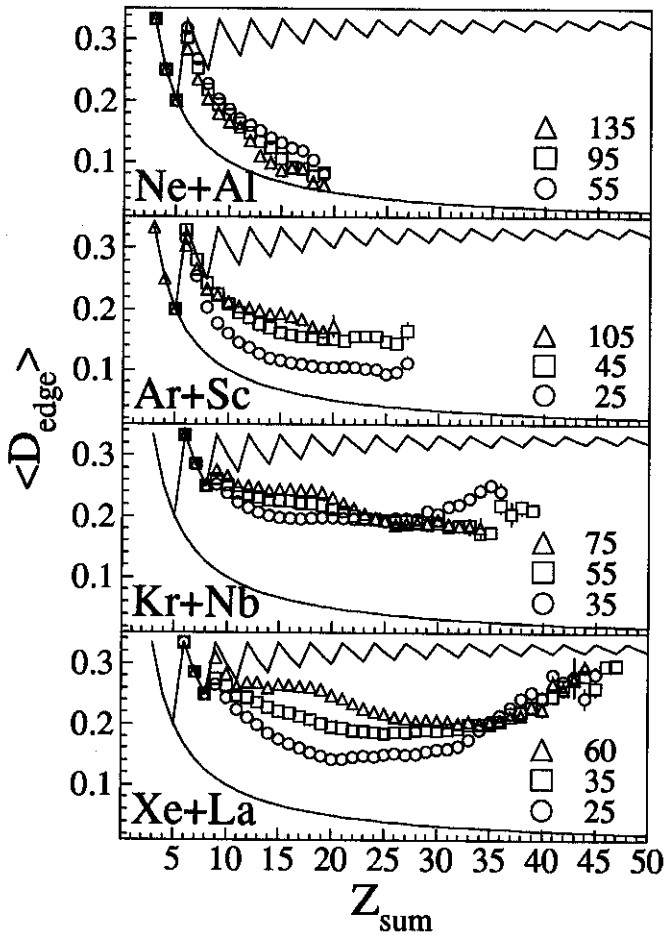

Figure 2: The average values of D_{edge} versus Z_{sum} in the central events for three representative beam energies in MeV/nucleon for each entrance channel, as labeled. The solid lines indicate the minimum and maximum values of D_{edge} that are possible for each value of Z_{sum} by definition.

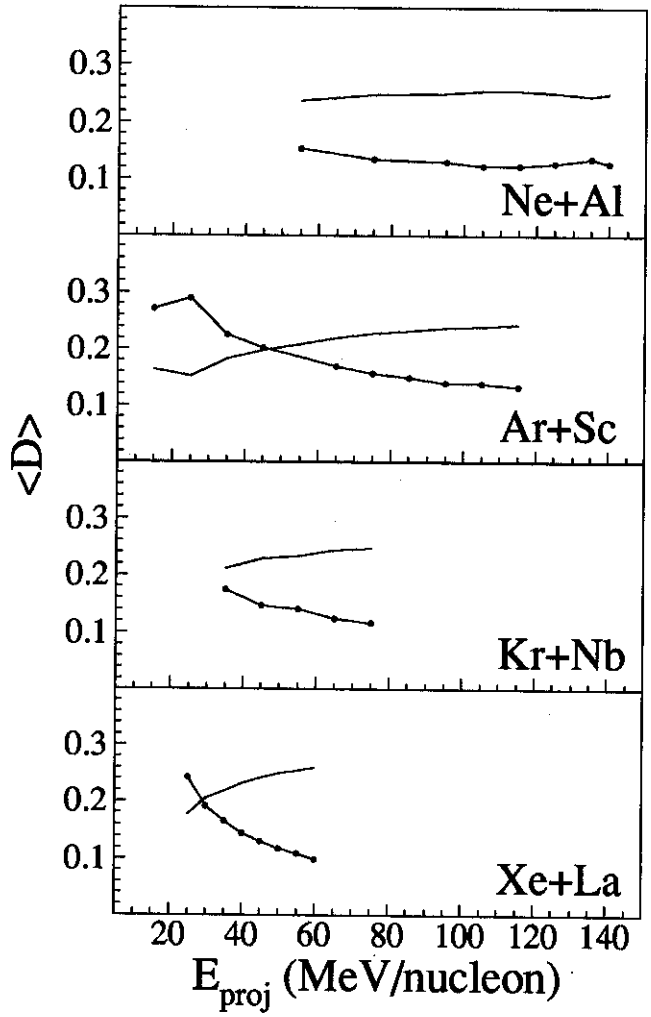

Figure 3: The average values of D_{cent} (with points) and D_{edge} (without points) versus the beam energy for specific gates on the quantity Z_{sum}: $6 \leq Z_{sum} \leq 17$ for the ^{20}Ne+^{27}Al and ^{87}Kr+^{93}Nb entrance channels, and $6 \leq Z_{sum} \leq 20$ for the ^{40}Ar+^{45}Sc and ^{129}Xe+^{139}La entrance channels.

Figure 4: The average values of Z_{sum} (upper left frame) and D_{cent} (upper right frame) obtained from eight samples of events, each generated at a specific excitation energy for central ^{40}Ar+^{45}Sc reactions using the Berlin code. Each sample is boosted from the CM frame to the laboratory, and then filtered, for beam energies from 25 to 105 MeV/nucleon. Some points in the upper frames have been offset for clarity by the amounts shown to the right. The lower frame compares the excitation energy dependence of the unfiltered Berlin events with the beam energy dependence of the filtered Berlin events, using BUU calculations to relate the beam and excitation energies for central ^{40}Ar+^{45}Sc reactions.